Ultrastructure of Metamorphosis in *Hydractinia echinata*

**Virginia M. Weis and
Leo W. Buss**

Abstract

The fine structure of metamorphosis in the athecate hydroid, *Hydractinia echinata,* is described. Metamorphosis was induced in two ways: by exposing planulae to appropriate microflora and by temporary exposure to an ionic imbalance. Larvae induced to metamorphose by ionic imbalance differed considerably in behavior, but little in fine structure, from those induced by microflora. Metamorphosis was initiated by the discharge of nematocysts and loss of neurosensory cells, followed by secretion of mucus from gland cells and dense-staining granules from supportive cells. Associated with these events is a severe folding of the larva and permanent adherence of the larva to the substratum by its anterior end. Following movement of remaining gland cells across the mesoglea into the endoderm and movement of interstitial cells into the ectoderm, the metamorphosing planula extends tentacle rudiments and stolonal buds, eventually elongating into a primary polyp.

Introduction

Hydroids have traditionally served as model developmental systems for the study of biological pattern formation. The ease with which many solitary forms, e.g., *Hydra,* can be manipulated via grafting and cell removal experiments has led to the establishment of widely discussed theories of pattern formation (Gierer and Meinhardt 1972). Such theories focus on the interacting influences of diffusible morphogens, which differentially influence cell growth and differentiation as a function of the distance from a source. In contrast to studies on the polypoid stage of the hydroid life cycle, studies of pattern formation during metamorphosis are all but lacking. Indeed, the ultrastructure of metamorphosis has only been described in one species to date (Martin et al. 1983). We here report on the ultrastructure of metamorphosis of the athecate hydroid *Hydractinia echinata* in response to induction by both ionic imbalance and by microflora, documenting the principal changes in planula behavior, size and shape, cell content, activity, migration, and differentiation. Pattern formation during metamorphosis is compatible with a mechanical interpretation based on the influence of changes in cellular composition and content on the viscoelastic body wall.

Materials and Methods

Study Species

Hydractinia echinata typically occurs as an epibiont of gastropod shells occupied by

pagurid hermit crabs. *Hydractinia* larvae are induced to settle by bacteria of the genus *Alteromonas* (Müller 1969, 1973; Spindler and Müller 1972). The presence of the appropriate microflora appears obligate, as metamorphosis does not occur in its absence (Müller 1973, Yund et al. 1987). Bacterial induction of metamorphosis, however, can be mimicked by a brief exposure to artificially high concentrations of certain monovalent cations (Spindler and Müller 1972, Müller 1973, Berking 1984).

Matings

Hydractinia is a dioecious hydroid (Hauenschild 1954) whose spawning is initiated in response to light (Bunting 1894, Ballard 1942). Laboratory-cultivated or field-collected colonies were placed in aerated dishes overnight and fertilized eggs were collected the following morning. Planulae competent to settle developed within 18–24 hours at room temperature. All planulae were used for observations within 96 hours after fertilization.

Induction of Metamorphosis by Microflora

Planulae were added to culture bowls containing the hermit crab *Pagurus longicarpus* occupying shells of the gastropod *Urosalpinx cinerea*. Planulae adhering to freshly collected shells began metamorphosis within one hour of their initial contact with the shell. Samples for fine structural analysis were removed for fixation at sequential stages over a 24–36 hour period. Repetition of these procedures using autoclaved shells fail to yield settlement and metamorphosis (Yund et al. 1987), indicating that the observed pattern of metamorphosis was indeed induced by the microflora inhabiting the shell.

Use of natural substrates as surfaces for settlement generates two difficulties. First, natural substrata are coated with debris and necessarily introduce debris in micrographs. The second difficulty is that removal of the planulae from the shell for sectioning may obscure detail in the zone of attachment. We,

nevertheless, feel that these disadvantages are far outweighed by the advantages of observing the process of metamorphosis under natural conditions.

Induction of Metamorphosis by Ionic Imbalance

Metamorphosis was induced via ionic imbalance by placing planulae in 0.55 mM CsCl, the salt concentration reported to have the greatest inductive effect (Spindler and Müller 1972). Specimens were removed for fixation every half hour from 1 to 4 hours after immersion in CsCl. After 4 hours remaining samples were removed from the CsCl solution to seawater. Planulae left in CsCl solutions for longer periods die; those left for shorter periods frequently resume characteristic planular morphology and fail to metamorphose (Spindler and Müller 1972, Müller 1973, Berking 1984, personal observation). Specimens were fixed at periodic intervals until metamorphosis was completed (24–48 hours).

Specimen Preparation

Specimens were fixed for 2 hours at room temperature in 4% glutaraldehyde in 0.1 M sodium cacodylate-buffered, double strength, filtered seawater at pH 7.0, rinsed in buffer for 3 successive 10-minute washes and then post-fixed in 2% OsO_4 in 0.1 M sodium cacodylate buffered, double strength, filtered seawater. After a second series of three 10-minute washes in buffered seawater, specimens were dehydrated in an ethanol series. Specimens for transmission electron microscopy (TEM) were infiltrated with propylene oxide and embedded with a Spurr's epoxy mixture at 70° C overnight. Blocks were sectioned on a Huxley ultramicrotome, stained with uranyl acetate and Reynold's lead citrate, and viewed with a Philips 300 series transmission electron microscope. Specimens for scanning electron microscopy (SEM) were fixed and dehydrated as described above, critical point dried in a Polaron critical point dryer with CO_2, mounted on stubs, sputter-

Table 1

Summary of cell types found during metamorphosis of *Hydractinia echinata*.

GERM LAYER	CELL TYPE	INDUCTION TYPE	PLANULA	EARLY METAMORPHOSIS	LATE METAMORPHOSIS	PRIMARY POLYP
Ectoderm	Supportive cell		Ciliated, columnar	Some ciliated, columnar	Not ciliated, cuboidal	Not ciliated, spindle shape
	Apical vesicles	Microfloral	Yes	Yes	Few	No
		Ionic imbalance	—	Yes	Yes	No
	Basal vesicles	Microfloral	Few	Yes	Yes	No
		Ionic imbalance	—	Few	Yes	No
	Gland cell	Microfloral	Yes	Yes	Few*	No
		Ionic imbalance	—	Yes	Yes*	No
	Nerve cell	Microfloral	Yes	Yes	Yes	Yes
		Ionic imbalance	—	Yes	Yes	Yes
	Sensory cell	Microfloral	Yes	Few	No	No
		Ionic imbalance	—	Few	No	No
	Nematocyte	Microfloral	Yes	Yes*	Yes*	Yes
		Ionic imbalance	—	Few*	No	Yes
	Cnidoblast	Microfloral	Yes	Yes	Yes	Yes
		Ionic imbalance	—	Yes	Yes	Yes
	Interstitial cell	Microfloral	No	No	Few**	Yes
		Ionic imbalance	—	Few	Yes**	Yes
Endoderm	Endodermal cell	Microfloral	Yes	Yes	Yes	Yes
		Ionic imbalance	—	Yes	Yes	Yes
	Cnidoblast	Microfloral	Yes	Yes	Yes	Yes
		Ionic imbalance	—	Yes	Yes	Yes
	Interstitial cell	Microfloral	Yes	Yes	Yes	Yes
		Ionic imbalance	—	Yes	Yes	Yes
	Gland cell A	Microfloral	No	No	Few	Yes
		Ionic imbalance	—	No	Few	Yes
	Gland cell B	Microfloral	No	No	Few	Yes
		Ionic imbalance	—	No	Few	Yes

* At anterior end only.
** At posterior end only.
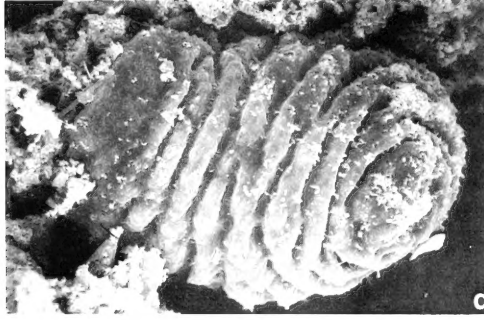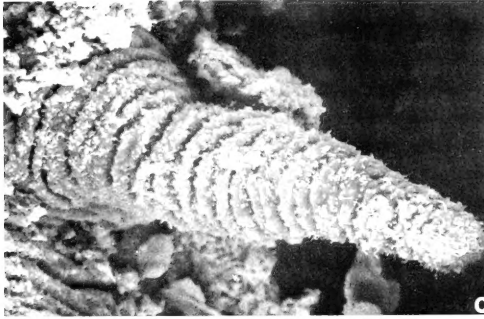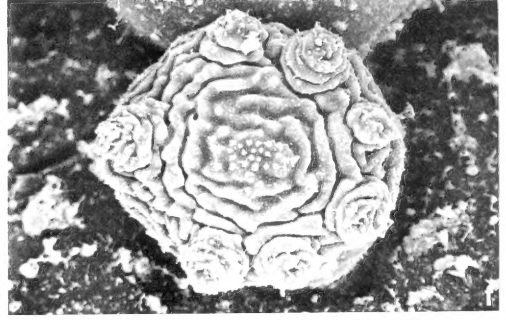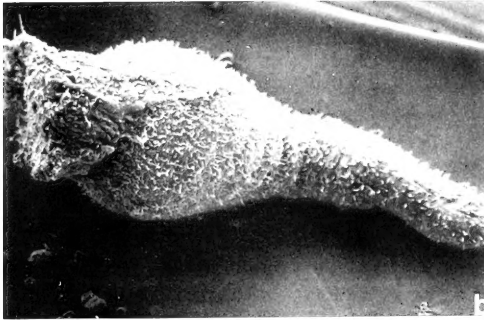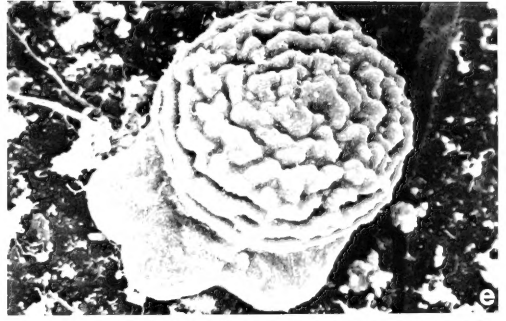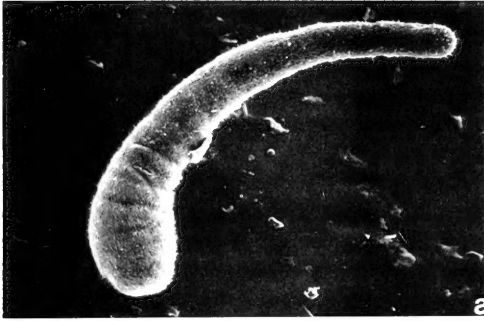
coated with gold-paladium, and viewed with an ISI SS-40 scanning electron microscope.

Cell Type Quantification

Low magnification (350–1000×) micrographs of the planulae were produced to quantify gland cell density. The number of cells was counted directly and the area of the micrograph measured, using a Summagraphics bit-pad interfaced to an Apple II+ microcomputer, in 10 sections for each of the first 5 hours after the onset of metamorphosis.

Results

Results of the two treatments are presented separately. The ultrastructure of the mature planula larva of *Hydractinia* is well documented (Weis et al. 1985) and information about planula structure is included here only to form a basis for description of alterations in structure occurring during metamorphosis. The occurrence of each cell type throughout metamorphosis is summarized in Table 1.

Metamorphosis Induced by Microflora

Gross Morphology and Behavior (Fig. 1). Planulae crawl along the surface of the

shell for some 10–60 minutes following their initial contact. Movement is typically restricted to regions immediately surrounding the site of initial contact. After crawling ceases, the planula, 500–600 μm in height, assumes an upright position with the blunt anterior end in contact with the substratum (Fig. 1a). The larva coils its tapered posterior tip around its anterior end and remains in this posture for approximately 30 minutes. The planula then begins to contract (Fig. 1b, c). The process of contraction and folding continues for 3–5 hours, the larva eventually collapsing onto itself to produce a highly convoluted, flattened cone, 100–130 μm in height and 100–120 μm in basal diameter (Fig. 1d). The larva remains in this state for 5–7 hours, followed by production of stolonal buds (Fig. 1e) and tentacle rudiments (Fig. 1f). Basal development and tentacle formation are frequently asynchronous (Fig. 1e, f). Basal development involves the proliferation of a uniform ectodermal mat (Fig. 1e) or the elongation of individual stolons or both (Fig. 1h). Stolonal buds and ectodermal mat are sheathed in a loose, finely convoluted mucous sheath (Fig. 1g). Tentacle buds appear in a ring surrounding the top of the nearly spherical polyp (Fig. 1f). As the tentacles elongate, cnidocils become apparent on the surface of the tentacles and hypostomal regions, while the polyp itself elongates to assume a typical adult morphology over the next 12–24 hours (Fig. 1h).

◀ **Fig. 1**
Microfloral induction treatment. Scanning micrographs of the larva at sequential stages of metamorphosis upon hermit crab shells. a) Planula prior to the onset of metamorphosis. Note attachment to the substratum with the blunt anterior tip (96×). b) Planula during the 1st hour in the coiled stage. The posterior end of the larva has been uncoiled to reveal the character of underlying ectoderm. Notice the extracellular matrix secreted from the anterior end (154×). c) Planula during the 2nd hour of metamorphosis. The blunt end is securely attached to the substratum and the tapered end has begun to fold (246×). d) Planula in the 5th hour of metamorphosis. The tapered end has continued to contract, forming an aciliate, flattened cone (373×). e) Developing polyp after approximately 12 hours of metamorphosis. Note early development of the ectodermal mat. f) Developing polyp after 12–14 hours of metamorphosis. Notice that tentacle rudiments have formed, that mature nematocytes are visible in the tentacles and the developing hypostome, and that this specimen lacks early development of an ectodermal mat (260×). g) Primary polyp after 24–48 hours. Tentacles have elongated with little basal development (202×). h) A fully mature primary polyp with tentacles and stolons (182×).
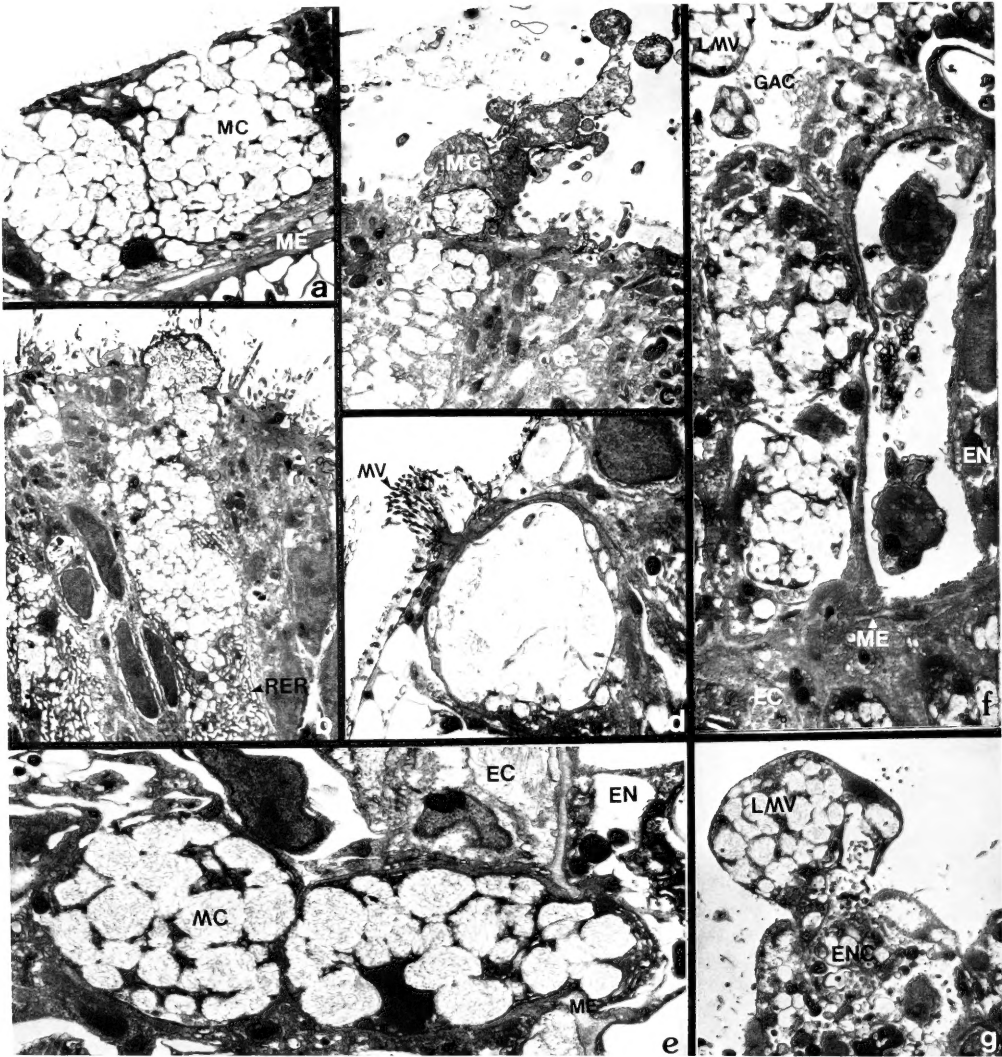
Fig. 2

Gland cell. a) Gland cells prior to the onset of metamorphosis (3631×). b) Swollen apex of the cell and extensive RER in the base of the cell during the 1st hour of metamorphosis (3000×). c) An apical extension of gland cell membrane during the 1st hour of metamorphosis (5349×). Note that the membrane of a mucous vesicle in the center of the micrograph is ruptured and that the vesicle's contents are found both within the vesicle and in the surrounding seawater. d) Gland cell, 3 hours after the onset of metamorphosis, emptied of its mucous vesicles (6507×). e) Gland cell protruding through the mesoglea, 4 hours after the onset of metamorphosis (6545×). f) Gland cells on opposite sides of the mesoglea in the 4th hour of metamorphosis. Note that one gland cell in the endoderm has lysed. Fragments of gland cells can be seen in the gastric cavity (4104×). g) Fragment of a gland cell associated with apical cell membrane of an endodermal cell (4104×). EC = ectoderm, EN = endoderm, ENC = endodermal cell, GAC = gastric cavity, LMV = lysed mucous vesicle, ME = mesoglea, MC = mucous (gland) cell, MG = mucous vesicle, MV = microvilli, RER = rough endoplasmic reticulum.

Fine Structure of Ectoderm   The mature planula larva is characterized by five ectodermal cell types: neurosensory cells, gland cells, epitheliomuscular cells (EMC), nematocytes, and nerve cells. During metamorphosis, the ectoderm of the planula retains the EMC, nerve cells, and some nematocytes, loses the gland and neurosensory cells, and acquires interstitial cells.

Neurosensory Cell.   Neurosensory cells, found clustered at the tapered end of the planula, are characterized by an abundance of dense-cored neurosecretory vesicles, one or more Golgi complexes, a medially located nucelus, and a short cilium emergent on the ectodermal surface (Weis et al. 1985). The neurosensory cell disappears when the larva adopts a coiled posture at the onset of metamorphosis.

Gland Cell (Figs. 2, 3).   Ectodermal gland cells, concentrated at the anterior end of the planula, are characterized by large, tightly packed electron-lucent granules, a dense-staining basal nucleus, and a centrally placed cilium encircled by a basket of microvilli (Fig. 2a). The gland cell displays marked changes in structure and content early in metamorphosis, disappears from the ectodermal surface in late metamorphosis, and is absent in the primary polyp.

Gland cell structure is considerably altered at the onset of metamorphosis, while the larva is still coiled. The microvillar net is everted, and portions of the apical membrane are extended (Fig. 2a, b). These extensions of the apical membrane are populated by mucous vesicles (0.9–1.3 μm in diameter) which protrude from the cell membrane into the surrounding water column (Fig. 2c). Protruding vesicles at the surface-water interface are either found intact or display ruptures of the vesicle membrane, with vesicle contents seen both within the vesicle itself and in the surrounding water column (Fig. 2c). Gland cell microvilli, which encircle the cilium in the mature larva (Fig. 2a), are elongated and are deployed in a disorganized fashion surrounding extensions of the apical membrane. Gland cells lacking mucous
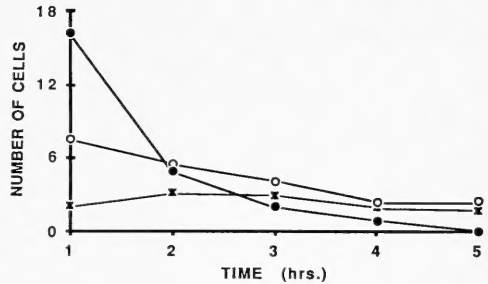

Fig. 3
Density of gland cells with everted microvilli as a function of time at three locations on the ectodermal surface of the planula. Data represent means of 10 sections. Paired T-tests show that cell densities differ significantly in the 1st hour (P < 0.05), but are not significantly different at all later stages of metamorphosis. Closed points = anterior end, open circles = longitudinal axis, asterisks = posterior end.

vesicles, but still possessing a cilium and microvilli, appear at this time (Fig. 2d).

Throughout the early hours of metamorphosis, there is a dramatic increase in the quantity of rough endoplasmic reticulum (RER) present in the gland cell (Fig. 2b). Beginning at the 3rd hour of metamorphosis, openings in the otherwise continuous mesoglea appear adjacent to gland cells along the longitudinal axis of the planula and at the posterior end. Gland cells are found extending through these openings (Fig. 2e). At this time, cells, identical to ectodermal gland cells in cell size, vesicle size, and cell shape, are first observed in the endoderm (Fig. 2f). By hours 4–5 of metamorphosis, no gland cells are found in the ectoderm at the anterior end and few are seen at the tapered tip (Fig. 3). At this time, gland cells in the endoderm are often found lysed and numerous large mucous vesicles are found free-floating within the developing gastric cavity. These mucous vesicles frequently appear in association with apical membranes of endodermal cells (Fig. 2f, g).

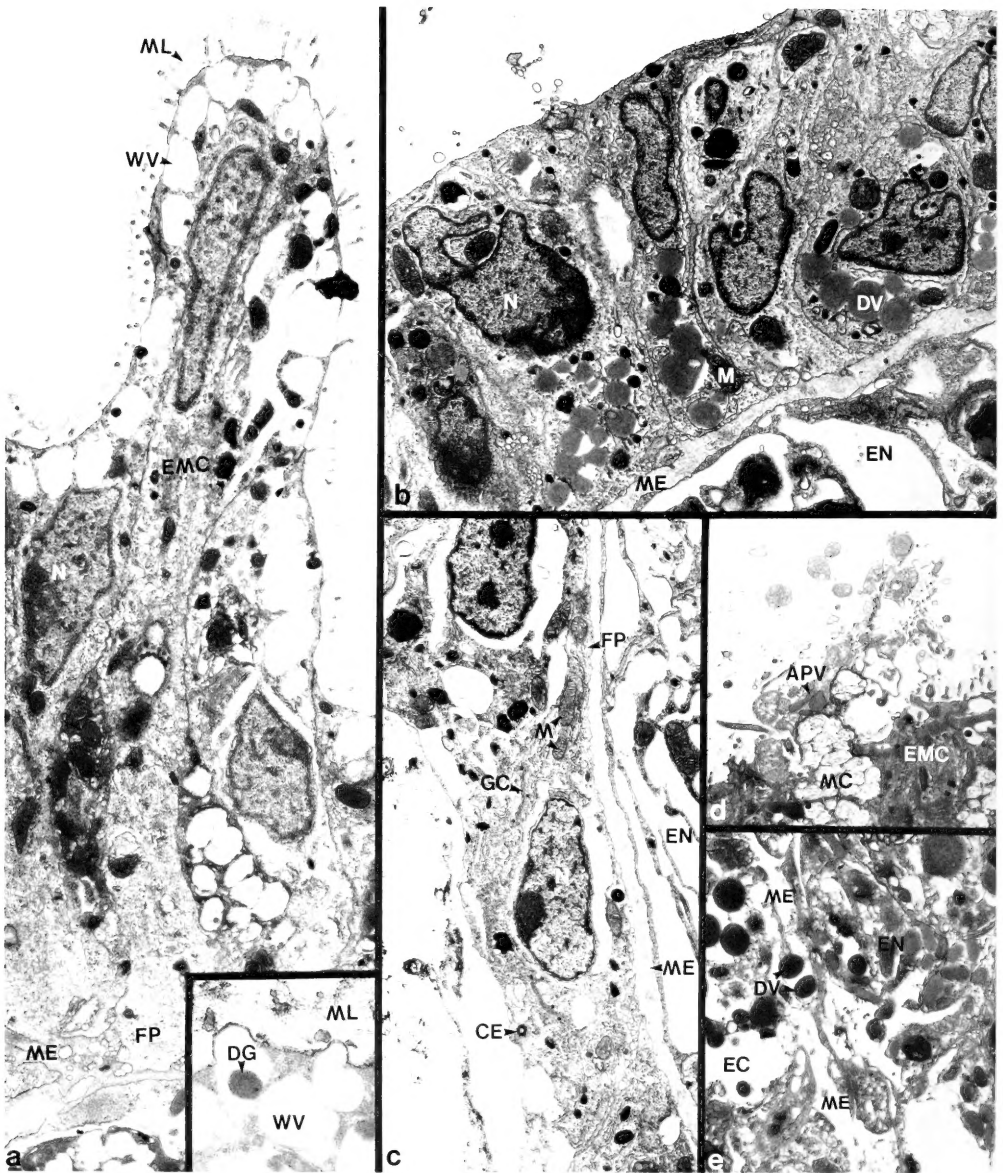**Supportive Cell** (Fig. 4).   The supportive

Fig. 4

Epitheliomuscular cell. a) EMC near the posterior end during the 3rd hour of metamorphosis. Note numerous white vacuoles, some with dense cores (inset) arrayed at the ectodermal surface of the cell (9223×; inset 16,680×). b) Cuboidal EMCs at the anterior end of the larva late in metamorphosis. Note the large vesicles present at the base of the cells (6178×). c) Spindle-shaped EMC in the primary polyp, with muscular processes extending along the mesoglea (5600×). d) Dense-staining granules at the apical end of an EMC associated with gland cell vesicles during the 1st hour of metamorphosis (16,680×). e) Dark-staining vesicles at opposite sides of the endoderm and ectoderm during the 2nd hour of metamorphosis (5666×). APV = apical vesicle, CE = centriole, DG = dense-staining granule, DV = dark-staining basal vesicle of EMC, EMC = epitheliomuscular cell, FP = foot process of EMC, GC = Golgi complex, M = mitochondrion, ML = mucous layer, N = nucleus, WV = white vacuole. Other labels as described in previous figures.

cell of the planula larva extends from the ectodermal surface to the mesoglea and is characterized by a large medial nucleus, a Golgi complex, numerous mitochrondria, a single cilium, muscular processes, and several apical, dense-staining, membrane-bound granules. The mitochrondria, Golgi complex, rough endoplasmic reticulum (RER), and muscular processes remain unaltered in relative position and appearance throughout metamorphosis (Fig. 4a). Striking modifications, however, are seen in EMC size, shape, ciliation, and the position and content of intracellular vesicles during metamorphosis.

During the initial stages of metamorphosis, many EMCs lack cilia and by 5 hours after initiation of metamorphosis, the entire planula is aciliate (Figs. 1d, 4a, c). Supportive cell shape and size alters throughout metamorphosis. EMCs located at the anterior end of the planula are reduced in height in early stages of metamorphosis, as the posterior end of the planula collapses upon the base (from 32.3 ± 2.5 μm in length from base to apex in the planula to 23 ± 1.7 μm). EMCs eventually adopt a cuboidal shape in the base of the newly metamorphosed polyp and in developing stolonal buds (Fig. 4b, EMC length 13 ± 2.0 μm). Along the longitudinal axis of the metamorphosing larva, the cell is also smaller, eventually becoming spindle-shaped and oriented parallel to the mesoglea in the elongating primary polyp (4–6 μm in height, Fig. 4c).

Dense-staining granules (mean, 0.6 μm in diameter), found throughout the cytoplasm of the mature planula, appear adjacent to the apical membrane during the first 2 hours of metamorphosis (Fig. 4d). Apical granules of the EMC appear in close proximity to gland cell vesicles and, like the vesicles of gland cells, are found both within fine protrusions of the cell's apical membrane and in the surrounding water column (Fig. 4d). Few of these apical granules remain in later stages of metamorphosis. Apical granules are often associated with numerous small white vacuoles, averaging 0.81 μm in diameter (range: 0.51–1.3 μm), along the entire ectodermal surface (Fig. 4a). These vacuoles,

containing small dense-staining granules, (0.24–0.41 μm in diameter) appear as projections from the surface of the cell membrane (Fig. 4a, insert). While the dense-staining granules are lost during metamorphosis, the apical vacuoles are retained through the late stages of metamorphosis into the adult polyp.

Large, round, dark-staining, basal vesicles (mean: 0.8 μm in diameter; range: 0.6–1.2 μm), found only rarely in the ectoderm of the mature planula, begin to appear in large quantities within EMCs in the anterior end of the larva during the second hour of metamorphosis (Fig. 4b). At this same time, identical vesicles are found clustered at the base of endodermal cells (Fig. 4e) and, occasionally, embedded within the mesoglea itself. These vesicles become increasingly dense in the cytoplasm of ectodermal EMCs as metamorphosis proceeds, eventually becoming concentrated in apical regions. Vesicles are lost as the larva adopts a cone shape, 5–6 hours after onset of metamorphosis.

Interstitial Cells (Fig. 5a–c).   Interstitial cells (I-cells), found only in the endoderm of the mature planula, are nearly spherical and characterized by a large nucleus (3.8–4.0 μm in diameter), mitochrondria, a uniformly staining cytoplasm rich with polysomes, and few other discernable organelles (Fig. 5a). Interstitial cells first appear in the ectoderm at the 4th hour of metamorphosis, at which time I-cells can be found extending through the mesoglea at the anterior end of the planula (Fig. 5b). I-cells reside at the base of the ectoderm along the mesoglea, often occurring in clumps of 3–4 cells. During the final stages of metamorphosis, interstitial cells are found in highest densities in basal regions of the polyp and the developing ectodermal mat (Fig. 5c).

Nematocytes (Fig. 5d, e).   Mature nematocytes, clustered at the tapered posterior tip of the mature planula, are characterized by mitrochrondria, dense streams of microfilaments, a Golgi complex, RER, and capsules of either atrichous isorhizas or desmonemes capped with a cnidocil. Many mature nematocytes discharge
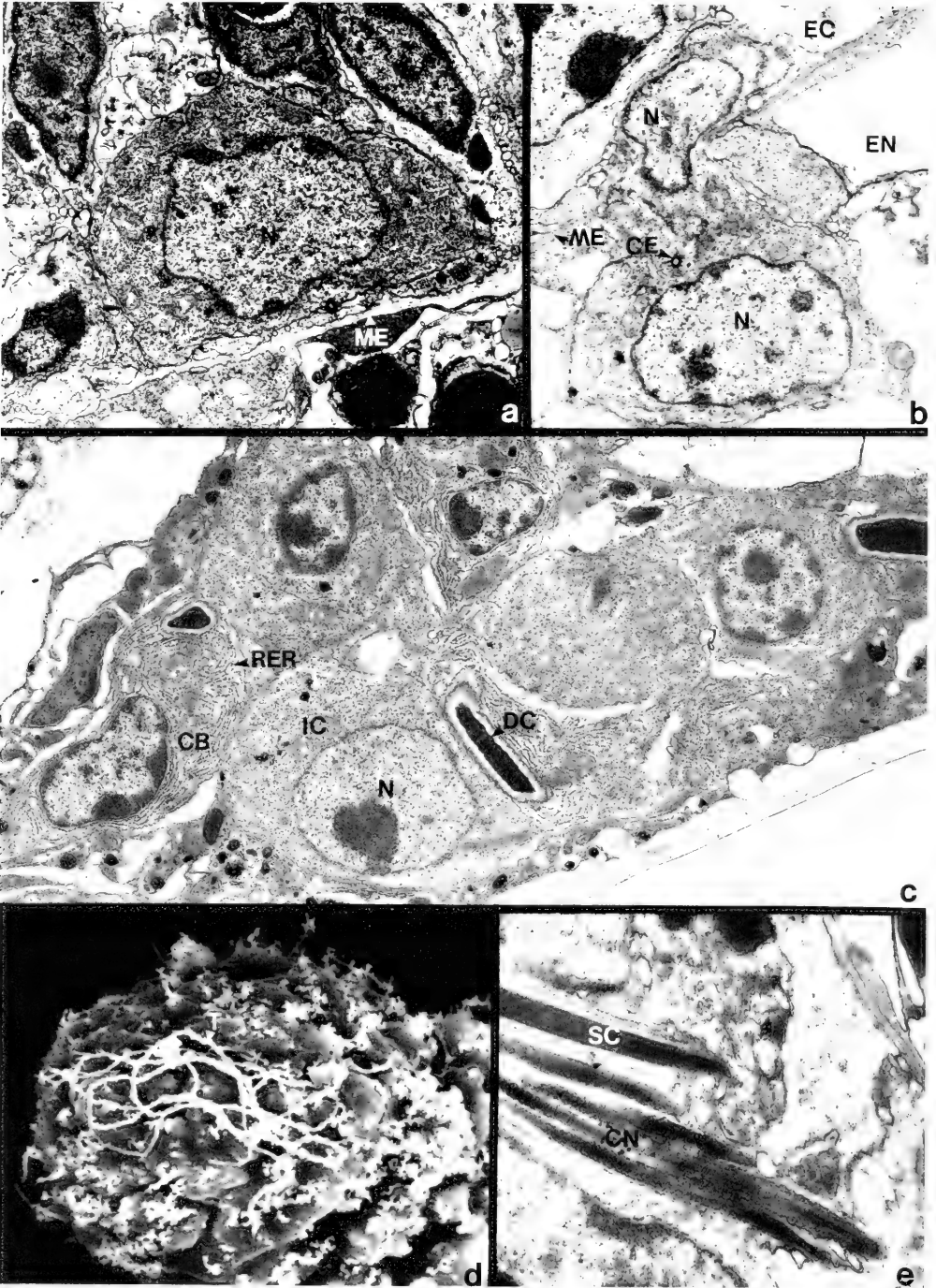
in early stages of settlement and those remaining are found in markedly different orientations during subsequent stages of metamorphosis.

Discharged nematocytes are found coating the posterior ectodermal surface of the planula following the initial attachment of the planula to the shell (Fig. 5d). Mature nematocytes disappear from the ectodermal surface at this stage. At this time, fully mature nematocytes, complete with cnidocil (Fig. 5e), appear at the base of the ectoderm oriented parallel to the mesoglea (Fig. 5e). These cells remain unaltered in cell structure and contents throughout the metamorphosis process.

At late stages of metamorphosis, both cnidoblasts and mature nematocytes are found in those folds of the ectoderm destined to develop into tentacle buds. Cnidoblasts in the early stages of differentiation are also found in the base of the developing polyp and ectodermal mat (Fig. 5c). As tentacles mature, nematocytes appear in their characteristic orientation perpendicular to the mesoglea and cnidocils are seen projecting from the ectodermal surface of the elongating tentacle buds (Fig. 1f–h).

Nerve Cell.   The nerve cell of the planula is oriented parallel to the mesoglea and is characterized by an irregularly shaped nucleus surrounded by perikaryon, neurites which extend along the mesoglea, mitochrondria, a prominent Golgi complex, microtubules, and irregularly occurring neurosecretory granules (Weis et al. 1985). The nerve cell retains the same position, cellular structure, and organization that it possesses in the planula throughout metamorphosis.

Fine Structure of the Endoderm

The endoderm of the metamorphosing larva contains endodermal cells, interstitial cells, cnidoblasts, and two types of gland cells (A and B). Interstitial cells and cnidoblasts display no features unique to their position in the endoderm and are not discussed further.

Endodermal Cell (Fig. 6).   A large endodermal cell, $14-16$ μm in length, is found oriented perpendicular to the mesoglea. The cell is characterized by a typically ovoid nucleus, $4.5-5$ μm in length, small amounts of RER, and numerous large vacuoles, $2.0-3.5$ μm in diameter, of variable content (Fig. 6a). Some vacuoles often contain large electron-transparent crystals throughout metamorphosis (Fig. 6b). During the early stages of metamorphosis, other vacuoles are often found containing large, dark-staining, round vesicles approximately 0.8 μm in diameter. These vesicles are identical in size and structure to those appearing in the basal cytoplasm of ectodermal EMCs at the same time (Figs. 4e, 6c). Endodermal cells acquire large vesicles, $4.5-5$ μm in diameter, late in metamorphosis, at the time at which gland cells disappear from the ectoderm, with contents closely resembling the mucous vesicles of the ectodermal gland cell (Figs. 2f, g, 6a).

Gland Cells (Fig. 6).   Two endodermal gland cells (Fig. 6d), absent from the mature planula, first appear in the developing hypostome in the 6th–7th hour of metamorphosis. Both cell types are columnar, averaging 10.2 μm in length (range: $7.5-13.5$ μm), and characterized by a basally located

◀ **Fig. 5**
Nematocyte and interstitial cell. a) Interstitial cell (I-cell) at the base of the ectoderm 6 hours after the onset of metamorphosis. b) I-cell protruding through the mesoglea in the 5th hour of metamorphosis ($7062\times$). c) Basal region of the primary polyp containing an abundance of I-cells and cnidoblasts ($5042\times$). d) Scanning micrograph of the posterior end of a planula in the 2nd hour of metamorphosis, bearing threads of discharged nematocysts on the ectodermal surface ($1248\times$). e) Cnidocil of a mature nematocyte lying parallel to the mesoglea in the 4th hour of metamorphosis ($16\,393\times$). CB = cnidoblast, CN = cnidocil, DC = developing capsule of a nematocyst, IC = interstitial cell, SC = stereocilium, T = nematocyst thread. Other labels as described in previous figures.
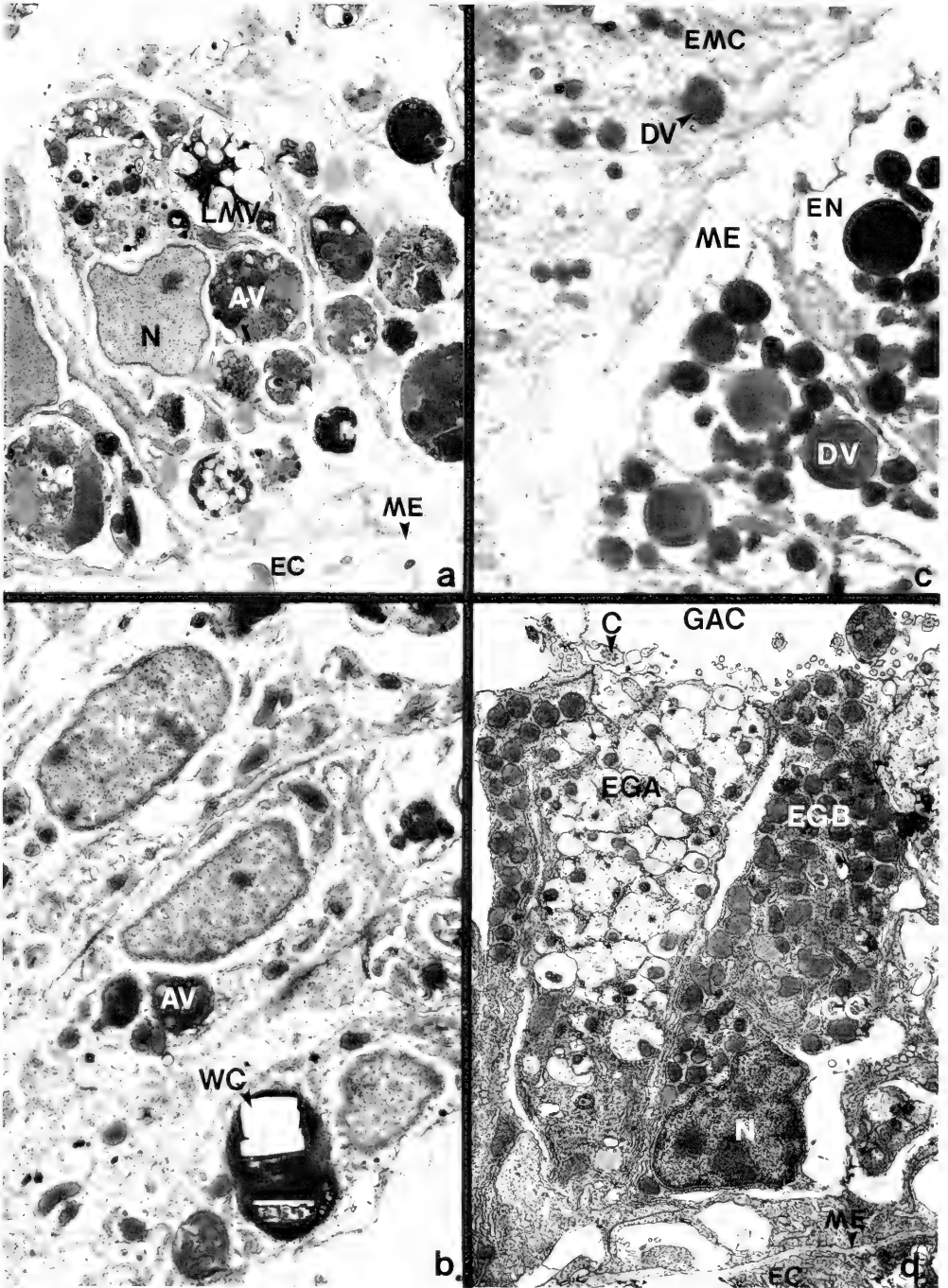
nucleus, 2.3–2.6 μm in diameter, a Golgi complex lying above the nucleus, mitochondria clustered at the base of the cell, and often a large quantity of RER. Both cells possess a cilium with associated microvilli that extend into the opening gastrovascular cavity. The two cells are distinguished on the basis of intracellular granules. Type A gland cells contain tightly packed electron-lucent granules, averaging 0.70 μm in diameter (range: 0.51–0.92 μm), with dark-staining cores, 0.2–0.3 μm in diameter. Type B gland cells contain dark-staining vesicles, averaging 0.41 μm in diameter (range: 0.37–0.55 μm), that are less densely packed than those of type A. Endodermal gland cells A and B (8.5–13.5 μm) become reduced in height during late metamorphosis to reach a final dimension of 6.5–9.0 μm in the young polyp.

Metamorphosis Induced by Ionic Imbalance

The discussion of metamorphosis by ionic induction is limited only to those changes unique to this treatment. In all other details, results are as described for the microflora treatment.

Gross Morphology and Behavior (Figs. 7–9)   The planula alternates between crawling along the substratum and temporarily adhering to the surface of the culture bowl with its blunt anterior end (Fig. 7a). After immersion in CsCl, both the morphology and behavior of the larva undergo pronounced changes. Immediately following immersion, a fibrous extracellular matrix (Fig. 8a, b) begins to cover the larva, first concentrated at the

anterior end of the larva and later progressing along the longitudinal axis of the larva to eventually cover the posterior tip in a continuous sheath (Fig. 8c, d). Within 1 hour, the planula begins to contract (from 500–600 μm to 350 μm) and adhere to the surface along its longitudinal axis (Fig. 7b) or by the tapered posterior tip (not shown). The anterior end of the larva, characterized by a distinct dimple in the mature planula (Weis et al. 1985), has everted to form a convex anterior pole (Figs. 7b, 8a). After 2.5 hours, the planula contracts further (Fig. 7c), but has lost its sheath of mucus (Fig. 9a–d) and is no longer adhesive. After 4 hours, the posterior tip of the planula is severely folded, reducing the planula to a third of its original length (200 μm, Fig. 7d). The larva again becomes highly mobile, gliding over the substratum with its blunt anterior end forward. Planulae placed in seawater at this time retain their nearly spherical state (Fig. 7e) and begin metamorphosing over the following 12–48 hours. The spherical larva broadens in the region corresponding to the former position of the anterior pole (Fig. 7f) and develops a slight centrifugal constriction below which develop stolonal buds and above which form tentacle buds (Fig. 7g). These structures elongate to assume the typical polypoid morphology (Fig. 7h).

Fine Structure   Three of the 6 ectodermal and all of the endodermal cell types display no obvious alterations in fine structure as a consequence of immersion in the CsCl solution. The behavior of the gland cell, the nematocyte, and the EMC are modified. The principal differences between the microflora

◄ **Fig. 6**
Endodermal cells. a) Endodermal cell in late stage of metamorphosis containing vacuoles and a mucous vesicle, resembling that of ectodermal gland cells (2975×). b) Endodermal cells at the base of the gastric cavity of a primary polyp. Note the vacuole containing large, white crystals (5058×). c) Large dark-staining vesicles in the endoderm pressing up against the mesoglea in the 3rd hour of metamorphosis. A single vesicle resides in an EMC across the mesoglea in the ectoderm (5349×). d) Endodermal gland cells A and B in the hypostomal region of a primary polyp (3333×). AV = vacuole, C = cilium, EGA = endodermal gland cell type A, EGB = endodermal gland cell type B, WC = white crystal. Other labels as described in previous figures.
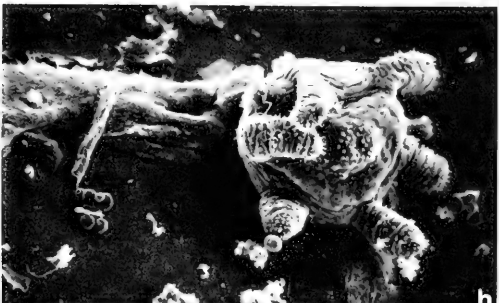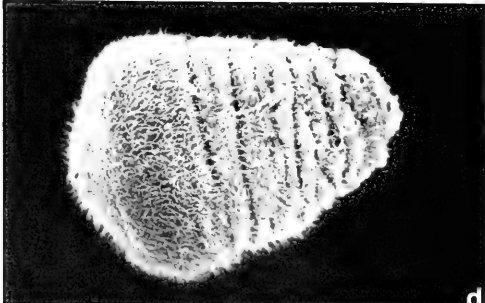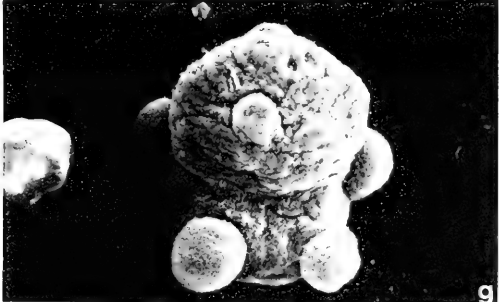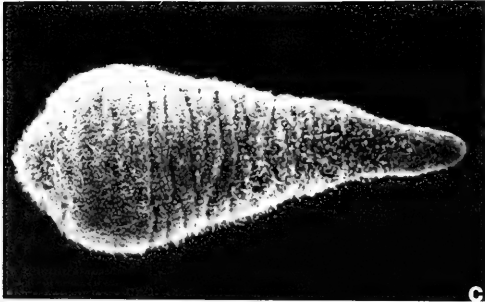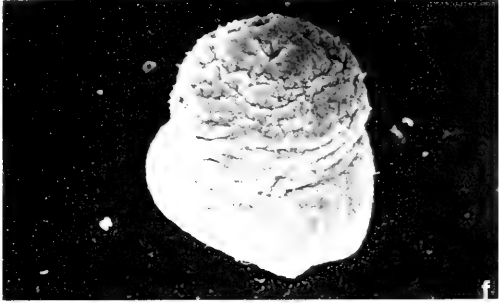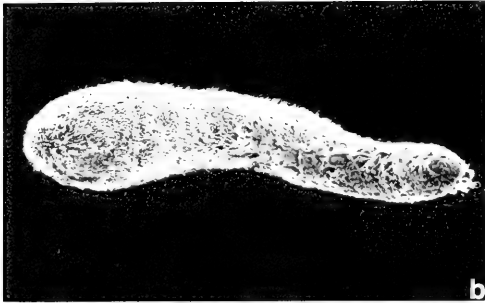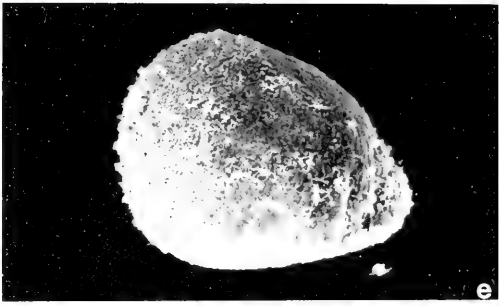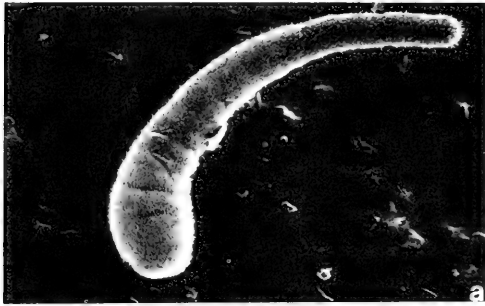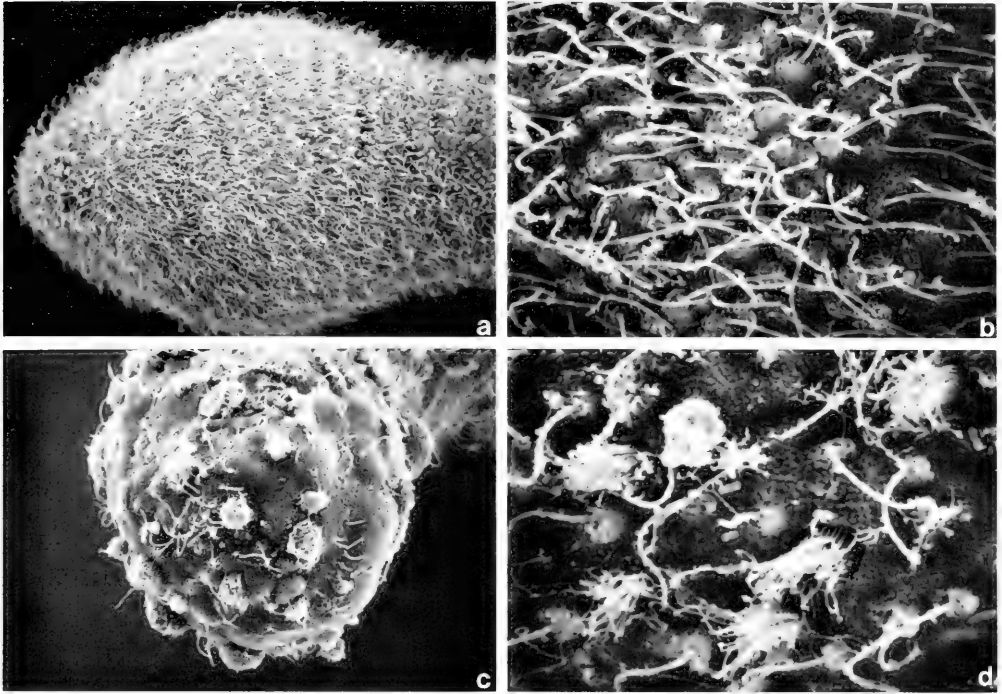
Fig. 8

Scanning micrographs of planulae after 1 hour in CsCl. a) The anterior end of a planula (539×). b) A higher magnification of the anterior end showing the fibrous extracellular matrix covering the cilia (2926×). c) The posterior end covered in a thick slime coat (466×). d) Magnification of the anterior edge of the slime coat showing where the fibrous matrix becomes layered into the thick, even sheath (2926×).

treatment and the ionic imbalance treatment are manifested in the relative timing and extent of changes in cell structure and position already detailed above, rather than in novel events. We do not provide micrographs of identical changes differing only in their relative timing and/or extent.

Gland Cell. Gland cells, immediately upon immersion in CsCl, display the eversion of the microvillar cavity and loss of gland cell contents observed in microflora induction. Virtually all gland cells of the larva display this structure. The loss of mucous vesicles is temporally correlated to the appearance of the mucous sheath (Figs. 7b, 8) and period of adhesiveness. Gland cells are lost from the larval ectoderm, but, unlike the microflora treatment, this loss is not associated with the

◀ **Fig. 7**

CsCl induction treatment. Scanning micrographs of planulae at sequential stages of metamorphosis. a) Planula prior to the onset of metamorphosis (96×). b) Planula after 1 hour in CsCl. The tapered tip is covered by a thick slime coat (180×). c) Planula after 2–3 hours in CsCl. Note that the larva has begun to contract and that it has everted the dimple at the anterior end (206×). d) Contracted planula after 4 hours in CsCl. (240×). e) Nearly spherical, aciliate planula after being removed from CsCl and placed in clean seawater for 12 hours (293×). f) Developing polyp (204×). g) A young polyp with both stolon and tentacle buds (220×). h) Primary polyp with stolon and tentacles 36–72 hours after the onset of metamorphosis. The tentacles and hypostome are studded with nematocytes (226×).
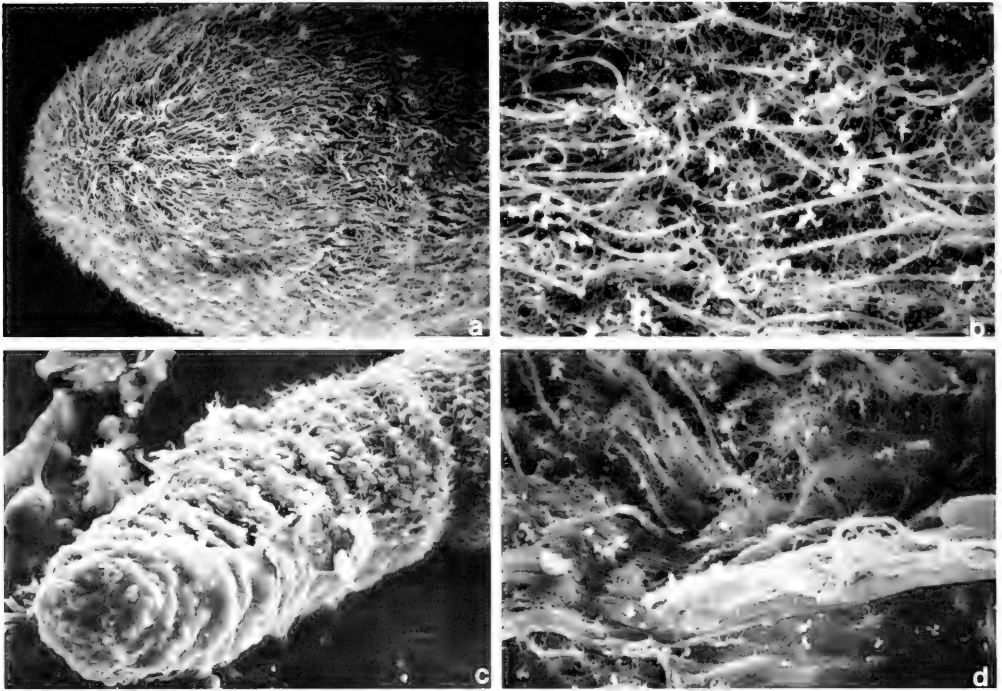
Fig. 9
Scanning micrographs of planulae after 2–3 hours in CsCl. a) The anterior end of a planula, showing the b) absence of the extracellular matrix seen earlier (1993×). Note the everted dimple (400×). c) The posterior end of the planula, now lacking a slime coat, showing gland cells with everted microvilli (713×). d) Magnification of the elongated microvilli of gland cells (2933×).

appearance of pores in the mesoglea or the subsequent appearance of gland cells in the endoderm. Relative to microflora induction, gland cell loss in CsCl is much more rapid. Just as gland cell eversion is associated with the appearance of the mucous sheath and a period of adhesiveness, the loss of gland cells is associated with the loss of the sheath and the period of resumed mobility.

Nematocytes.   All mature nematocytes are lost from the larval ectoderm upon immersion in CsCl. In contrast to the microfloral treatment, mature nematocytes are not found parallel to the mesoglea in early stages of metamorphosis. Cnidoblasts in varying stages of maturation, however, begin to appear in the ectoderm at this stage. Fully mature nematocytes are not found until the final stages of metamorphosis (Fig. 7f).

Supportive Cell.   As the larva shrinks in size during its exposure to CsCl, the cytoplasm of the EMCs becomes progressively disorganized. Upon removal to seawater, the EMC soon resumes its typical appearance. The dense-staining apical granules are lost only after the larva has been removed from CsCl and placed in seawater. The relative timing of this event is in stark contrast to that seen in the microfloral treatment (Fig. 4d), where EMC apical vesicles are lost at the same time as gland cells lose their contents.

Discussion

The process of metamorphosis in *Hydractinia* may be conveniently divided into four stages,

dominated sequentially by (1) cell loss, (2) cellular secretions and permanent attachment to the substratum, (3) folding of the body wall and associated cell movements, and (4) production of tentacle rudiments and formation of the primary polyp. A summary of the principal activities during each stage follows.

Stage 1

Shortly after contact with the shell, the larva loses all neurosensory cells and the majority of its nematocytes. These cells appear to function in the process of habitat selection. The mature *Hydractinia* larva adheres to sand grains by its anterior end with its posterior tip extending over the sediment-water interface (Weis et al. 1985). Hence, the posterior tip of the larva, where both neurosensory cells and nematocytes are clustered (Weis et al. 1985), is first exposed to the activities of passing hermit crabs. The observation of discharged nematocysts after initial attachment of the planula (Fig. 5d) and the disappearance of mature nematocytes from the ectodermal surface is consistent with the suggestion of several investigators that the function of nematocysts is to hoist the crab onto the shell (Lyons 1973, Müller et al. 1976, Chia and Bickell 1978, Martin et al. 1983). The function of neurosensory cells is obscure. They may either direct the discharge of nematocytes or sense the presence of inducing bacterial species, or both (see Müller 1973).

Stage 2

Shortly after the loss of nematocytes and neurosensory cells, gland cells and EMCs begin to lose the vesicles and granules they contain. The release of these substances appear to adhere the larva to the substratum. Several lines of evidence suggest that gland cells secrete mucous vesicles onto the shell surface. First, mucous vesicles are clearly seen at cell-water interfaces and have been captured in the process of releasing their contents into the surrounding water column (Fig. 2c). Second, gland cells emptied of

mucous vesicles are found in increasing frequency as metamorphosis proceeds (Fig. 2d). Third, the loss of mucous vesicles is associated with the eversion of the complex microvillar basket (Fig. 2b, d), a process known to be associated with mucous release in anthozoans (Chia and Koss 1983). Finally the eversion of microvilli can be seen on the surface of the planulae in SEM (Fig. 9c, d) and occurs at precisely the time that the surface becomes covered with a mucous sheath (Fig. 7b).

The secretion of mucous vesicles is temporally associated with increased adhesiveness of the larva. In the CsCl treatment, the mucus first appears at the anterior pole of the larva, comes to coat the entire planula, and finally concentrates at the posterior pole (Fig. 8). This progression is mirrored by patterns of adhesion. The larva is first found adhering by its anterior end, followed by adhesion along its longitudinal axis, and subsequently by its posterior tip. Furthermore, with the loss of mucus from the surface (Fig. 9), the larva is no longer adhesive and resumes its mobile habit. The loss of most gland cells after the discharge of their contents, and their failure to reappear at later stages of metamorphosis, strongly suggests that the function of these cells is the deployment of the contents of the adhesive mucous vesicles themselves. Gland cell substances, though adhesive (Bodo and Bouillin 1968, Martin et al. 1983), do not produce permanent attachment of the larva to the substratum, as indicated by the ability of planulae to resume their mobile habit subsequent to the release of gland cell substances in the CsCl treatment.

As the gland cells are lost and the larva becomes embedded in the mucus they secrete, EMCs begin to lose dense-staining granules from their cytoplasm. The facts that such granules are found dispersed throughout the cytoplasm in the mature planulae, are concentrated at the apical end at the onset of metamorphosis, become associated with vacuoles protruding from the apical cell membrane (Fig. 4a), and are lost from the apical membrane as metamorphosis proceeds

(Fig. 4d), strongly imply that the granules are secreted. The loss of dense-staining granules is temporally associated with permanent adhesion of the larva to the substrate in both treatments. In the microfloral treatment, the EMC granules are released into an extracellular environment rich in gland cell secretions (Fig. 2c). In the CsCl treatment, however, granule release occurs in the absence of obvious gland cell secretion, at a time when the vast majority of the gland cells have already been lost. The fact that the larva permanently adheres to the surface in the absence of mucous secretions strongly suggests that the dense-staining apical granules are required for permanent attachment.

Stage 3

The third stage of metamorphosis is characterized by the severe folding of the larva and several associated cell movements. The folding of the larva appears to be associated with the loss of cells in earlier stages of metamorphosis. Folding first occurs at the posterior tip, corresponding to the position of those cells which are first lost. As metamorphosis proceeds, folding occurs over the entire length of the larva as gland cells begin to disappear (Figs. 1, 7). Finally, folding occurs much more rapidly in CsCl (2.5 hours) than in the microfloral treatment (5 hours), as would be predicted by the more rapid loss of gland cells in this treatment.

Various cells, found in stereotypic positions in the mature larva, display changes in their relative positions during this period. Gland cells are observed extending through holes in the mesoglea at this time (Fig. 2e) and first appear within the endoderm (Fig. 2f). Once in the endoderm, gland cells appear to lyse, as evidenced by the observation of numerous mucous vesicles found free-floating in the developing gastric cavity (Fig. 2f). At this same time, mucous vesicles are found in association with the apical membranes of endodermal cells (Fig. 2g) and mucous vesicles first appear within large vacuoles in the cytoplasm of endodermal cells (Fig. 6a).

The absence of such vacuoles prior to gland cell transport and lysis strongly imply that endodermal cells are autophagic and that the function of gland cell transport is the transfer of unused mucous vesicles to endodermal cells. I-cells are first seen in the ectoderm at this time. The appearance of holes in the otherwise continuous mesoglea adjacent to these cells and the observation of I-cell types protruding through the mesoglea at the time at which I-cells first appear in the ectoderm suggests active transport (Fig. 5b).

Stage 4

After contraction of the larva, a fluted ring of tentacle primordia appears on the heretofore amorphous larva (Fig. 1f). Cnidoblasts and mature nematocytes migrate to these rudiments. The mesoglea, rent at various points at earlier stages, is continuous. Shortly thereafter, the larva expands from its highly folded state to adopt the form of the primary polyp (Fig. 1g, h).

Mechanical Model of Hydroid Metamorphosis

The sequence of events described for the metamorphosis of *Hydractinia* larvae suggests a hypothetical model of hydroid metamorphosis, based on the cascading influences of an initial cell loss on the viscoelastic body wall. At the onset of metamorphosis, most cells lacking permanent fibrillar anchors in the mesoglea are lost. The loss of nematocytes, neurosensory cells, and gland cells has mechanical consequences. These ectodermal cells are oriented perpendicular to the mesoglea, a viscoelastic body wall composed of fibrillar collagen in an aqueous matrix (Gosline 1971a, 1971b). The loss of the various ectodermal cells leaves the mesoglea largely populated by EMCs, whose muscular processes are embedded within the mesoglea (Fig 4c). As cells are lost, these muscular processes remain unaltered. Hence the mesoglea is placed under tension at points of muscular insertion and under

compression at points of cell loss. Such a deformation of a viscoelastic material likely produces the horizontal folds seen in the collapsing larva (Fig. 1). As the larva contracts, ruptures appear in the otherwise continuous mesoglea. Those cells which lie adjacent to these holes are pressed through them, gland cells into the endoderm and I-cells into the ectoderm (see Figs. 2e, 5b). As the larva collapses onto the substratum, it produces a fluted ring of tentacle primordia (see Fig. 1f). The formation of a fluted ring of tentacles on the compressed larvae is consistent with the behavior of shear forces acting within the larva. As D'Arcy Thompson (1942) first suggested, if the collapse of the posterior tip of the larva onto its adherent base generates a splashlike deformation of the mesoglea, then structures resembling tentacle rudiments would be produced (see Fig. 1f). Those cells residing in the ectoderm unattached to the mesoglea, largely cnidoblasts and nematocytes (Fig. 4e), would be forced into regions of most rapid flow, generating tentacles bearing nematocytes. Finally, the collapse of the larva brings the ruptured ends of the mesoglea into contact and the well-known capacity of collagen to adhere to itself may act to reestablish a continuous body wall. This body wall would, however, still be deformed. The expansion of the mesoglea to form a primary polyp is characteristic of the behavior of a viscoelastic membrane following deformation. The viscoelastic mesoglea possesses a characteristic resting state, such that an equilibrial size will be regained by the substance upon deformation (Chapman 1953, 1959, Hausman and Burnett 1969, Alexander 1962, Gosline 1971a, 1971b). The larval mesoglea, originally deformed as a consequence of cell loss, may necessarily expand to an upright posture of the polyp as a mechanical consequence of the original deformation (see Fig. 1f, g). While these mechanical interpretations are highly speculative, the ease with which the ultrastructure of metamorphosis accords with a simple mechanical model suggests that mechanical consequences of deformation of the viscoelastic body wall is an important force shaping hydroid pattern formation.

Acknowledgments

Literature Cited

Alexander, R. 1962. Viscoelastic properties of the body wall of sea anemones. J. Exp. Biol. 39:373–86.

Ballard, W. W. 1942. The mechanism of synchronous spawning in *Hydractinia* and *Pennaria*. Biol. Bull. 82: 329–39.

Berking, S. 1984. Metamorphosis of *Hydractinia echinata*: Insights into pattern formation in Hydroids. Wilhelm Roux' Arch. Dev. Biol. 193:370–78.

Bodo, F. and **J. Bouillin.** 1968. Etude histologique du développement embryonnaire de quelques hydroméduses de Roscoff: *Phialidium hemisphaericum* (L.), *Obelia sp.* Peron et Lesueur, *Sarsia eximia* (Allman), *Podocoryne carnea* (Sars), *Gonionemus vertens* Agassiz. Cah. Biol. Mar. 9:69–104.

Bunting, M. 1894. The origin of sex-cells in *Hydractinia* and *Podocoryne*. J. Morphol. 9:203–36.

Chapman, G. 1953. Studies on the mesogloea of Coelenterates. II. Physical properties. J. Exp. Biol. 30: 440–51.

———— 1959. Mesogloea of *Pelagia nectiluca*. Quart. J. Microsc. Sci. 100:599–610.

Chia, F. S. and **L. Bickell.** 1978. Mechanisms of larval settlement and the induction of settlement and metamorphosis: a review, p. 1–12. *In* F. S. Chia and M. E. Rice (eds.), Settlement and Metamorphosis of Marine Invertebrate Larvae. New York, Elsevier.

Chia, F. S. and **R. Koss.** 1983. On the fine structure of the nematocysts in the planula larva of a sea anemone *Anthopleura elegantissima*. Biol. Bull. Nat. Taiwan Normal Univ. 18:11–24.

Gierer, A. and **H. Meinhardt.** 1972. A theory of biological pattern. Kybernetik 12:30–39.

Gosline, J. M. 1971a. Connective tissue mechanics of *Metridium senile*. I. Structural and compositional aspects. J. Exp. Biol. 55:763–74.

———— 1971b. Connective tissue mechanics of *Metridium senile*. II. Visco-elastic properties and macromolecular model. J. Exp. Biol. 55:775–95.

Hauenschild, C. 1954. Genetische und entwicklungsphysiologische Untersuchungen über Intersexualitat und Gewebevertraglichkeit bei *Hydractinia echinata* Flem. (Hydrozoa, Bougainvillidae). W. Roux' Arch. Entwicklungsmech. Org. 147:1–41.

Hausman, R. E. and **A. L. Burnett.** 1969. The mesoglea of *Hydra*. I. Physical and histochemical properties. J. Exp. Zool. 171:7–14.

Lyons, K. M. 1973. Collar cells in planula and adult tentacle ectoderm of the solitary coral *Balanophyllia regia* (Anthozoa: Eusammiidae). Z. Zellforsch. 145:57–74.

Martin, V. J., F. S. Chia and **R. Koss.** 1983. A fine structural study of metamorphosis of the hydrozoan *Mitrocomella polydiademata*. J. Morphol. 176:261–87.

Müller, W. A. 1969. Auslösung der Metamorphose durch Bakterien bei den Larven von *Hydractinia echinata*. Zool. Jahrb. Anat. Bd. 86:84–94.

———— 1973. Induction of metamorphosis by bacteria and ions in the planulae of *Hydractinia echinata*: an approach to mode of action. Publ. Seto Mar. Biol. Lab. 20:195–208.

Müller, W. A., F. Weiker and **R. Eiben.** 1976. Larval adhesion, releasing substance, and metamorphosis, p. 347–54. *In* G. O. Mackie (ed.), Coelenterate Ecology and Behavior. New York, Plenum Press.

Spindler, A. N. and **W. A. Müller.** 1972. Induction of metamorphosis by bacteria and by lithium pulse in the larvae of *Hydractinia echinata* (Hydrozoa), Wilhelm Roux' Arch. Entwicklungsmech. Org. 169:271–80.

Thompson, D'A. W. 1942. On Growth and Form. Cambridge, Cambridge Univ. Press. 346 p.

Weis, V., D. R. Keene and **L. W. Buss.** 1985. Biology of hydractiniid hydroids. 4. Ultrastructure of the planula of *Hydractinia echinata*. Biol. Bull. 168:403–18.

Yund, P. O., C. Cunningham and **L. W. Buss.** 1987. Recruitment and post-recruitment interactions in the colonial hydroid *Hydractinia*. Ecology, in press.

The Authors

Virginia M. Weis. Department of Biology, University of California, Los Angeles, CA 90024.

Leo W. Buss. Department of Biology and Curator Invertebrate Zoology, Peabody Museum of Natural History, Yale University, New Haven, CT 06511.